Available online at www.sciencedirect.com
ScienceDirect
Mendeleev Commun., 2024, **34**, 107–109

Mendeleev Communications

Synthesis and photophysical activity of 6-substituted isocoumarins

Elena S. Fedina,[*a,b*] **Mikhail A. Arsenov,**[*a*] **Kseniya L. Isakovskaya,**[*a*]
Dmitry V. Muratov[*a*] **and Dmitry A. Loginov***[*a,c*]

[a] *A. N. Nesmeyanov Institute of Organoelement Compounds, Russian Academy of Sciences, 119334 Moscow, Russian Federation. Fax: +7 499 135 5085; e-mail: dloginov@ineos.ac.ru*
[b] *Sirius University of Science and Technology, 354340 Sochi, Russian Federation*
[c] *G. V. Plekhanov Russian University of Economics, 117997 Moscow, Russian Federation*

DOI: 10.1016/j.mencom.2024.01.032

6-Substituted isocoumarins with aryl, alkynyl, and diphenylamino substituents were synthesized from 4-bromobenzoic acid by annulation with tolane *via* rhodium-catalyzed C–H activation followed by palladium-catalyzed cross-coupling reactions. The compounds obtained exhibit luminescence emission in the violet–blue region (370–480 nm) with quantum yields up to 95% (for the diphenylamino derivative). Aggregation of biphenyl-substituted isocoumarin leads to a strong bathochromic shift (by 80 nm) of emission as a result of intermolecular π–π stacking interactions.

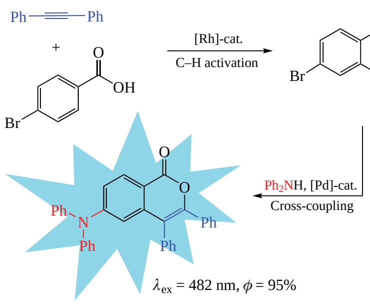

Keywords: C–H annulation, cross-coupling, isocoumarins, luminescence, homogeneous catalysis.

Isocoumarins are less studied than isomeric coumarins which are the well-known organic luminophores.[1–3] Nevertheless, they are also promising organic scaffolds for use in organic electronics.[4–6] They have found application in the construction of efficient OLEDs,[7] including TADF-emitters.[8] Meanwhile, isocoumarins usually act as acceptor moieties in organic luminophores due to the low energy of the LUMO orbital (*ca.* −1.5–2.0 eV).[8–10] The donor properties of isocoumarins can manifest themselves only in relation to stronger acceptors (for example, isoquinolinium cations), however, such cases are very rare.[11] Recently, we have shown that isocoumarins with strong electron-withdrawing substituents (such as CN, CF$_3$, CO$_2$Et, *etc.*) at position 6 exhibited aggregation-induced emission (AIE), but even in this case, the luminescence quantum yield did not exceed 15%.[10] Therefore, the introduction of donor substituents into the isocoumarin framework seems to be more promising for the creation of luminophores with a high quantum efficiency. In the course of our ongoing studies on the development of new organic luminophores,[12–14] herein we report on a facile synthesis of 6-substituted isocoumarins with aryl, alkynyl and diphenylamino substituents as well as an investigation of their photophysical behavior.

Transition metal-catalyzed C–H activation of benzoic acids and their subsequent annulation with alkynes proved to be one of the most efficient methods for the synthesis of isocoumarins.[15–18] This approach allows one to create an isocoumarin framework in one step with high atom economy. However, the synthesis of functionalized derivatives requires additional preparation of the corresponding benzoic acids or post-functionalization of simple isocoumarins. For example, Wu and Shang[19] demonstrated the utility of 6-bromoisocoumarin **1** as a useful precursor for the synthesis of 6-pyrene and 6-carbazole derivatives *via* Pd-catalyzed Suzuki and Buchwald–Hartwig cross-coupling, though without evaluation of their photophysical properties. Notably, compound **1** can be prepared directly in one step from commercial 4-bromobenzoic acid and tolane *via* the Ru-catalyzed reaction in 58% yield.[19,20] Using this two-step methodology, we prepared a series of 6-aryl-substituted isocoumarins **2a–f** in good yields (Scheme 1). Analogously, 6-alkynyl (**3a**,**b**) and 6-diphenylamino (**4**) isocoumarins were synthesized from **1** by the Sonogashira and Buchwald–Hartwig reactions (Scheme 2). We also improved the procedure for the synthesis of the starting compound **1** using rhodium complex [Cp*RhCl$_2$]$_2$ as a catalyst instead of the Ru-derivatives. Although rhodium is more expensive than ruthenium,[21] we were able to decrease the catalyst loading by a factor of five and improve the yield of **1** up to 97% in the larger scale (2 mmol) reaction.

Isocoumarins **2a–f**, **3a**,**b** and **4** are stable in air both in the solid state and in solutions. Their ^{1}H NMR spectra show a

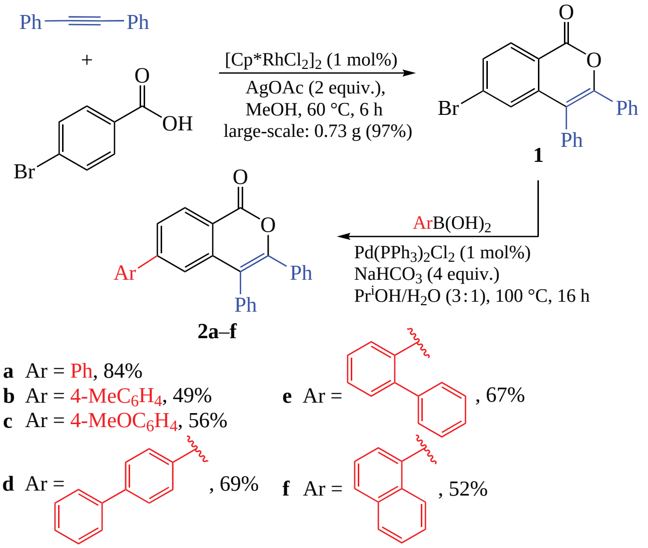

Scheme 1

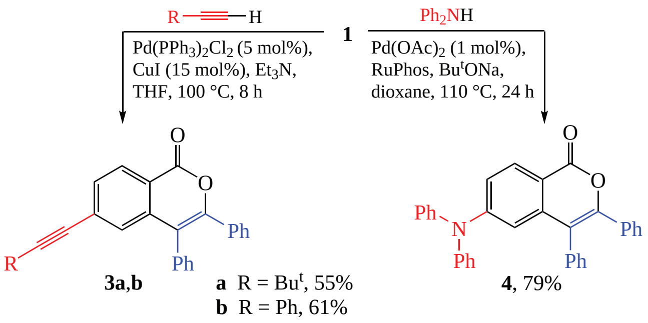

Scheme 2

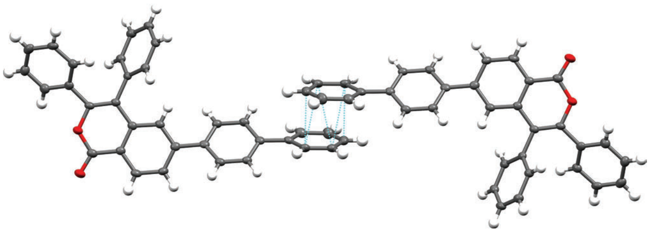

Figure 2 A fragment of the supramolecular chain of **2d**, showing intermolecular π–π stacking interactions.

doublet for the proton at position 8 (in the range δ 8.17–8.50 ppm) strongly downfield-shifted due to its proximity to the acceptor carbonyl group. This characteristic signal makes ^{1}H NMR spectroscopy informative enough for monitoring the reactant conversion and product purity. Moreover, its value proved to be strongly dependent on the nature of the substituent in position 6. For example, the replacement of the Ph substituent in **2a** with a strong donor NPh$_2$ group leads to an upfield shift from 8.46 to 8.17 ppm. In contrast, the IR spectroscopy did not give useful information, because isocoumarins showed the same strong absorption peak at 1737–1742 cm^{-1} (C=O) regardless of the substituents (see Online Supplementary Materials).

The structure of isocoumarin **2d** was confirmed by X-ray diffraction study (Figure 1).[†] There are two independent molecules in the crystallographic cell, which differ in the conformation of the biphenyl substituent relative to the isocoumarin framework (the latter is approximately planar for both molecules; the C(5)C(6)C(21)C(22) torsion angles for two independent molecules are equal to −32.5 or 47.5°, respectively). In the crystal, compound **2d** forms various short intermolecular contacts, including π–π stacking interactions between the terminal phenyl rings of biphenyl substituents in a tail-to-tail manner (Figure 2) with the intercentroid and shift distances of 3.980(7) and 2.156(6) Å, respectively.

To study the photophysical properties, absorption and fluorescence spectra in dichloromethane were measured (Table 1). All compounds demonstrate a long-wavelength absorption band ($S_0 \rightarrow S_1$) with maxima at 347–362 nm (for example, see Figure 3), which is mainly formed by the transition between HOMO → LUMO orbitals according to TD–DFT calculations at the B3LYP/6-31G(d) level (see Online Supplementary Materials). In most cases, this absorption corresponds to a $\pi \rightarrow \pi^*$ transition, because both frontier orbitals are delocalized at the phenyl substituent at position 3 and the isocoumarin moiety. The exception is compound **4** for which the HOMO orbital is located at the diphenylamine substituent leading to a charge-transfer transition. Nevertheless, compound **4** has the highest quantum yield (*ca*. 95%) of luminescence emission, while the quantum yields for other compounds do not exceed 10%. Interestingly, among aryl- and alkynyl-substituted isocoumarins linearly conjugated derivatives **2d** and **3b** have higher luminescence efficiency compared with other derivatives. Moreover, unlike other compounds, isocoumarin **2d** demonstrates an evident fine vibrational structure in the emission spectrum [Figure 4(*a*)] independently of the solvent nature (see Online

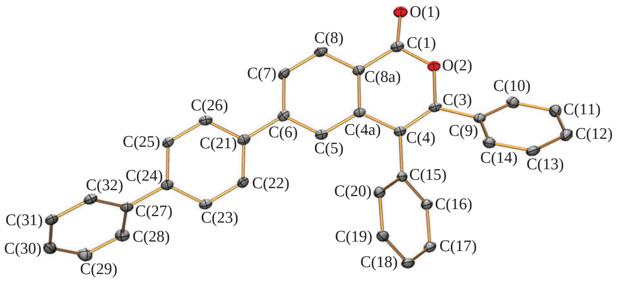

Figure 1 Molecular structure of **2d** in the representation of atoms as 50% probability ellipsoids; other symmetry-independent molecule and hydrogen atoms are omitted. Selected bond lengths for the shown symmetry-independent molecule (Å): O(1)–C(1) 1.206(3), C(1)–O(2) 1.378(3), O(2)–C(3) 1.392(3), C(3)–C(4) 1.344(3), C(4)–C(4a) 1.458(3), C(4a)–C(8a) 1.407(3), C(4a)–C(5) 1.402(3), C(5)–C(6) 1.385(3), C(6)–C(7) 1.404(3), C(7)–C(8) 1.382(3), C(8)–C(8a) 1.397(3), C(3)–C(9) 1.478(3), C(4)–C(15) 1.484(3), C(6)–C(21) 1.483(3).

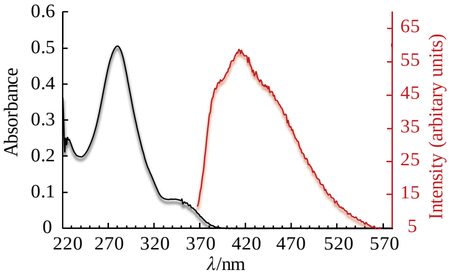

Figure 3 Absorption ($C = 1.7 \times 10^{-5}$ mol dm^{-3}) and emission ($C = 1.7 \times 10^{-5}$ mol dm^{-3}, λ_{ex} = 355 nm) spectra of **2a** in CH$_2$Cl$_2$.

Table 1 Absorptions and emission bands, as well as quantum yields for compounds **2a**–**f**, **3a**,**b**, and **4** in CH$_2$Cl$_2$.

Compound	λ_{abs}/nm (extinction coefficients ε)	λ_{em}/nm (λ_{ex}/nm)	ϕ (%) (λ_{ex}/nm)
2a	280 (29895), 347 (4672)	419 (355)	1.2 (292)
2b	287 (29404), 351 (3901)	422 (287)	1.3 (355)
2c	297 (29491), 358 (4113)	418 (297)	1.4 (355)
2d	300 (26256), 362 (2338)	373 (300)	9.8 (355)
2e	246 (19497), 285 (16302), 349 (3600)	416 (285)	1.2 (355)
2f	275 (23544), 300 (19353), 361 (2453)	425 (300)	2.0 (355)
3a	279 (31240), 317 (7556), 350 (4404)	418 (350)	1.7 (355)
3b	305 (36791), 361 (5126)	465 (300)	4.8 (355)
4	296 (32795), 350 (15821)	482 (350)	95.1 (355)

[†] *Crystal data for* **2d**. C$_{33}$H$_{22}$O$_2$ (M = 450.50), monoclinic, space group $P21/c$, at 100 K, a = 22.2865(8), b = 11.3753(4) and c = 18.0805(7) Å, β = 97.131(2)°, V = 4548.2(3) Å^3, Z = 8, d_{calc} = 1.316 g cm^{-3}, μ(MoKα) = 0.81 cm^{-1}, F(000) = 1888. A total of 46323 reflections were collected (8937 independent reflections, R_{int} = 0.0953) and used in the refinement, which converged to wR_2 = 0.1345 and GOOF = 1.037 for all the independent reflections [R_1 = 0.0581 was calculated for 6075 reflections with $I > 2\sigma(I)$]. Crystallographic data were collected with a Bruker Quest D8 CMOS diffractometer using graphite monochromated Mo-Kα radiation (λ = 0.71073 Å, ω-scans). Using Olex2,[22] the structure was solved with the ShelXT[23] structure solution program using Intrinsic Phasing and refined with the XL[24] refinement package using Least-Squares minimization against F^2 in anisotropic approximation for non-hydrogen atoms. The positions of hydrogen atoms were calculated and refined in the isotropic approximation in the riding model.

CCDC 2294584 contains the supplementary crystallographic data for this paper. These data can be obtained free of charge from The Cambridge Crystallographic Data Centre *via* http://www.ccdc.cam.ac.uk.

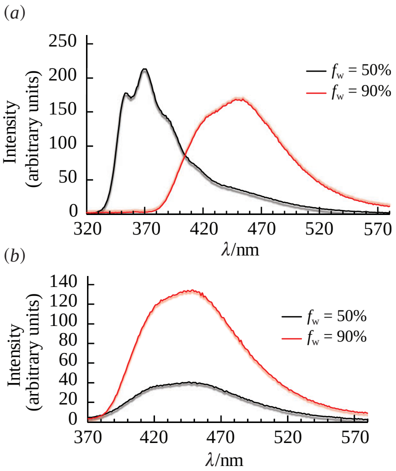

Figure 4 Emission spectra ($C = 2.4\times10^{-5}$ mol dm^{-3}, $\lambda_{ex} = 300$ nm) of (*a*) compound **2d** and (*b*) compound **2f** in H_2O/THF mixtures with different water content (f_w).

Supplementary Materials, Figure S15), which can be due to an increase in the contribution of the HOMO-1 → LUMO transition into the S_1 excited state. At the same time, the addition of water to a solution of **2d** in THF leads to a strong bathochromic shift (by 80 nm) of the emission band with loss of fine vibrational structure [see Figure 4(*a*)], which can be explained by the manifestation of intermolecular interactions in aggregates similar to those observed in crystals (see Figure 2).[25] Probably, intermolecular π–π stacking interactions between the terminal phenyl rings may prevent the HOMO-1 orbital from being involved into the S_1 excited state. Interestingly, in the case of naphthyl-substituted compound **2f** with an increase in water content (f_w) from 50 to 90 vol%, a 3-fold increase in emission was observed in the luminescence spectrum [Figure 4(*b*)]. The latter phenomenon can be explained either by the formation of excimers or by the AIE phenomenon, which may be caused by the restriction of intramolecular rotation of phenyl substituents or a decrease in the dihedral angle between naphthyl and isocoumarin moieties in aggregates.[26]

Finally, to explain the low luminescence efficiency of most aryl-substituted isocoumarins, we analyzed the difference in geometry of the ground state S_0 and the first singlet excited state S_1, which is mainly responsible for the fluorescence emission. It was found that in the case of the S_1 state of compound **2a**, there was a strong deviation of the ester oxygen atom from the cyclic plane, as well as an elongation of the C(1)−O(2) bond by 0.085 Å (Figure 5). This may indicate the occurrence of reversible electrocyclic ring opening of the lactone cycle with the formation of the corresponding ketene derivatives,[6,27] which can be considered as the main reason for the non-radiative decay. Notably, for isocoumarins **2d**, **3b**, and **4** with enhanced luminescence emission, the S_1 state retains the planar structure. The reversible nature of the ring opening reaction is indicated by the photostability of isocoumarin **2a** upon irradiation with $\lambda = 360$ nm in $CDCl_3$ during 24 h (according to ^{1}H NMR). Compounds **2d** and **4** also proved to be stable when irradiated under the same conditions.

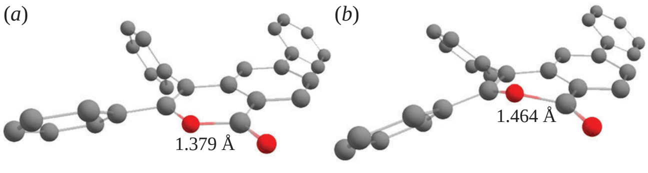

Figure 5 Geometries of (*a*) state S_0 and (*b*) state S_1 for isocoumarin **2a** optimized at the B3LYP/6-31G(d) level.

In summary, a facile synthesis of a series of new 6-substituted isocoumarins has been elaborated *via* a sequence of two transition metal-catalyzed reactions: C–H activation and cross-coupling. The simplest aryl-substituted compounds demonstrate very weak emission due to non-radiative decay caused by the low stability of the S_1 state, while linear biphenyl-, phenylethynyl- or amino-substituted derivatives are photostable and exhibit enhanced luminescence (quantum yield up to 95%).

This work was supported by the Russian Science Foundation (grant no. 17-73-30036). D.A.L. is also thankful to the Plekhanov Russian University of Economics for providing access to computation resources for DFT calculations. X-ray diffraction data were collected using the equipment of Center for molecular composition studies of INEOS RAS with the financial support from the Ministry of Science and Higher Education of the Russian Federation (contract/agreement no. 075-03-2023-642).

Online Supplementary Materials

Supplementary data associated with this article can be found in the online version at doi: 10.1016/j.mencom.2024.01.032.

References

1 M. Tasior, D. Kim, S. Singha, M. Krzeszewski, K. H. Ahn and D. T. Gryko, *J. Mater. Chem. C*, 2015, **3**, 1421.
2 D. Cao, Z. Liu, P. Verwilst, S. Koo, P. Jangjili, J. S. Kim and W. Lin, *Chem. Rev.*, 2019, **119**, 10403.
3 X. Sun, T. Liu, J. Sun and X. Wang, *RSC Adv.*, 2020, **10**, 10826.
4 M. A. Arsenov and D. A. Loginov, *INEOS Open*, 2021, **4**, 133.
5 T. Han, H. Deng, C. Y. Y. Yu, C. Gui, Z. Song, R. T. K. Kwok, J. W. Y. Lam and B. Z. Tang, *Polym. Chem.*, 2016, **7**, 2501.
6 A. A. Vidyakina, A. A. Shtyrov, M. N. Ryazantsev, A. F. Khlebnikov, I. E. Kolesnikov, V. V. Sharoyko, D. V. Spiridonova, I. A. Balova, S. Bräse and N. A. Danilkina, *Chem. – Eur. J.*, 2023, **29**, e202300540.
7 A. P. Molotkov, M. A. Arsenov, D. A. Kapustin, D. V. Muratov, N. E. Shepel’, Y. V. Fedorov, A. F. Smol’yakov, E. I. Knyazeva, D. A. Lypenko, A. V. Dmitriev, A. E. Aleksandrov, E. I. Maltsev and D. A. Loginov, *ChemPlusChem*, 2020, **85**, 334.
8 S. Qian, H. Zhang, J. Lan and Z. Bin, *Org. Electron.*, 2020, **84**, 105792.
9 V. Pirovano, M. Marchetti, J. Carbonaro, E. Brambilla, E. Rossi, L. Ronda and G. Abbiati, *Dyes Pigm.*, 2020, **173**, 107917.
10 M. A. Arsenov, Y. V. Fedorov, D. V. Muratov, Y. V. Nelyubina and D. A. Loginov, *Dyes Pigm.*, 2022, **206**, 110653.
11 M. A. Arsenov, D. V. Muratov, Y. V. Nelyubina and D. A. Loginov, *J. Org. Chem.*, 2023, **88**, 9360.
12 P. S. Gribanov, D. A. Lypenko, A. V. Dmitriev, S. I. Pozin, M. A. Topchiy, A. F. Asachenko, D. A. Loginov and S. N. Osipov, *Mendeleev Commun.*, 2021, **31**, 33.
13 P. S. Gribanov, D. V. Vorobyeva, S. D. Tokarev, D. A. Petropavlovskikh, D. A. Loginov, S. E. Nefedov, F. M. Dolgushin and S. N. Osipov, *Eur. J. Org. Chem.*, 2022, e202101572.
14 P. S. Gribanov, D. A. Loginov, D. A. Lypenko, A. V. Dmitriev, S. D. Tokarev, A. E. Aleksandrov, A. R. Tameev, A. Yu. Chernyadyev and S. N. Osipov, *Mendeleev Commun.*, 2023, **33**, 701.
15 T. Satoh and M. Miura, *Chem. – Eur. J.*, 2010, **16**, 11212.
16 M. P. Drapeau and L. J. Goossen, *Chem. – Eur. J.*, 2016, **22**, 18654.
17 D. A. Loginov and V. E. Konoplev, *J. Organomet. Chem.*, 2018, **867**, 14.
18 P. Saikia and S. Gogoi, *Adv. Synth. Catal.*, 2018, **360**, 2063.
19 J. Wu, B. Qian, Y. Liu and Y. Shang, *ChemistrySelect*, 2020, **5**, 10269.
20 S. Warratz, C. Kornhaaß, A. Cajaraville, B. Niepötter, D. Stalke and L. Ackermann, *Angew. Chem., Int. Ed.*, 2015, **54**, 5513.
21 A. A. Komarova and D. S. Perekalin, *Organometallics*, 2023, **42**, 1433.
22 O. V. Dolomanov, L. J. Bourhis, R. J. Gildea, J. A. K. Howard and H. Puschmann, *J. Appl. Crystallogr.*, 2009, **42**, 339.
23 G. M. Sheldrick, *Acta Crystallogr.*, 2015, **A71**, 3.
24 G. M. Sheldrick, *Acta Crystallogr.*, 2008, **A64**, 112.
25 S. Ma, S. Du, G. Pan, S. Dai, B. Xu and W. Tian, *Aggregate*, 2021, **2**, e96.
26 J. Me, N. L. C. Leung, R. T. K. Kwok, J. W. Y. Lam and B. Z. Tang, *Chem. Rev.*, 2015, **115**, 11718.
27 M. A. Kinder, J. Kopf and P. Margaretha, *Tetrahedron*, 2000, **56**, 6763.

Received: 19th September 2023; Com. 23/7252